The Report Committee for Chase Patrick Brown
Certifies that this is the approved version of the following Report

Improved Multidirectional Gaussian Mixture Models Applied to Probability of Collision of Resident Space Objects

APPROVED BY
SUPERVISING COMMITTEE:

_____
Ryan P. Russell, Supervisor

_____
Moriba K. Jah

Improved Multidirectional Gaussian Mixture Models Applied to Probability of Collision of Resident Space Objects

by

Chase Patrick Brown

Report

Presented to the Faculty of the Graduate School of

The University of Texas at Austin

in Partial Fulfillment

of the Requirements

for the Degree of

Master of Science in Engineering

The University of Texas at Austin

August 2020

To my patient wife.

Acknowledgements

Thank you to Dr. Ryan Russell for being my GN&C for these past two years of highly nonlinear motion and for teaching me you can take a partial derivative of anything if you code hard enough.

Thank you to Dr. Moriba Jah for your endless, brilliant musings on all things anthropogenic between us and the sun, as well as teaching me how you know who has the most accurate clock.

Thank you to Jason Stauch for teaching me that sometimes saying nothing is the best thing to say.

Abstract

Improved Multidirectional Gaussian Mixture Models Applied to Probability of Collision of Resident Space Objects

Chase Patrick Brown, MSE

The University of Texas at Austin, 2020

Supervisor: Ryan P. Russell

As the number of Resident Space Objects (RSOs) in Earth Orbit continues to rise by not only increased trackability but also an unprecedented number of commercial launches, conjunction assessment (CA) remains a paramount issue. Maintaining accuracy in probability of collision calculations is specifically of interest because any disparity will cause operators and analysts to lose trust, dismantling the entire CA system. Methods of state uncertainty propagation remain the most tractable way of controlling computational efficiency vs. accuracy. Gaussian Mixture Models (GMMs) have recently been used as an approach to maintain accuracy while decreasing the amount of computation time when compared to a Monte Carlo approach. These GMMs are able to represent the initial probability distribution function (pdf) as a weighted combination of individual Gaussian distributions. When propagated through a nonlinear function, such as the orbital equations of motion, higher order effects are maintained. How that initial pdf is split into a convolution of pdfs is the focus of this and current research. Multidirectional GMMs allow for the pdf to be split along directions of highest nonlinearity in a recursive manner. This study improves on this method by evaluating the directions at every split of every Gaussian mixture and also taking

into account the weight of that Gaussian mixture. Equinoctial elements are also explored as a potential element space to perform the splitting due their ability to maintain linearity during propagation. Results show that these improved methods are able to capture the majority of the nonlinear effects very well with relatively few GMs, and therefore can generate accurate Pc calculations, but fail to converge to the exact Monte Carlo value as more mixtures are added in a reasonable time. This is still of use to get within 5% of the Monte Carlo value with very few propagations in highly nonlinear encounters.

Table of Contents

List of Figures

Chapter 1: Introduction

Space Policy Directive 3 – The National Space Traffic Management Policy - has made it clear that "…on-orbit collision avoidance services is essential to preserve the space operational environment [1]." With the number of tracked objects in orbit expected to increase from about 25,000 to nearly 100,000 objects with the operational acceptance of the Space Fence [2,3], it is paramount that these collision avoidance services are timely, actionable, use all available data, and most importantly, are accurate. A loss of accuracy leads to a lack of trust; a lack of trust leads to poor decision making and, in this scenario, could lead to loss of assets, or even loss of life. Although there are many research avenues to support this realm, from dealing with multiple satellite state "opinions" from multiple providers [4] to "I've been told I have a probability of collision (Pc) with another satellite of 1 in a 1000 tomorrow morning…now what?", the focus of this study is on the accuracy portion. Accuracy is the cornerstone of probability of collision services, without it the entire structure crumbles. Uncertainty propagation remains one of the biggest sources of error. It is straight-forward to predict where a satellite's state will be some time in the near-future to some degree of confidence, given the appropriate force models. What is difficult is how does the initial uncertainty in that satellite's state move, stretch and grow as it is sent through the nonlinear orbital equations of motion? Is that "some degree of confidence" properly estimated? How precise is that solution? The current work explores these methods and makes improvements to increase accuracy and decrease computational costs.

1.1 Uncertainty Propagation

The initial uncertainty in a state can be represented as Gaussian distribution. Propagating through the nonlinear orbital equations of motion cause the uncertainty to

become more and more non-Gaussian, especially as more perturbations are added and time of propagation is increased. Successfully accounting for this evolution is paramount to conjunction assessment (CA) services because of the impact the final uncertainty plays in Pc calculations [5]. The uncertainty propagation methods explored are linear, unscented transforms, and Gaussian Mixture Models (GMMs).

1.1.1 Linear

Given an initial state $\boldsymbol{x_0}$ and initial covariance matrix $\boldsymbol{P_0}$, where the nonlinear orbital equations of motion are represented by

$$\boldsymbol{x}(t) = f(\boldsymbol{x_0}, t_0) \tag{1.1}$$

For the case of two body dynamics, the nonlinear function can be represented as an ordinary differential equation.

$$\dot{\boldsymbol{x}}(t) = \boldsymbol{F}\big(t, \boldsymbol{x}(t)\big) = \begin{bmatrix} \dot{\boldsymbol{r}}(t) \\ -\frac{\mu}{r^3}\boldsymbol{r}(t) \end{bmatrix} \tag{2.2}$$

The State Transition Matrix (STM) can be defined to propagate the deviation in the initial state to the deviation in the final state by linearizing the dynamics in a first order Taylor Series approximation where **x*** is a reference trajectory.

$$\Delta\boldsymbol{x}(t) = \boldsymbol{\Phi}(t, t_0)\Delta\boldsymbol{x}(t_0) \tag{3.3a}$$

$$\boldsymbol{\Phi}(t, t_0) = \left[\frac{\partial \boldsymbol{x}(t)}{\partial \boldsymbol{x}_0}\right]_{\boldsymbol{x}*} \tag{4.3a}$$

It can be shown [6] that the initial covariance $\boldsymbol{P_0}$ can be propagated to time t by

$$\boldsymbol{P} = \boldsymbol{\Phi}(t, t_0)\, \boldsymbol{P_0}\, \boldsymbol{\Phi}(t, t_0)^{\boldsymbol{T}} \tag{5.4}$$

Because higher order terms are truncated in the Taylor Series Expansion, higher order effects are not modeled in the dynamics. These terms can be included and State Transition

Tensors (STTs) can be used to propagate the uncertainty instead, but propagation of STTs require a large number of partial derivatives and suffer from the curse of dimensionality [7]. If an analytical expression for the STM can be derived, only one propagation of the state is required. If not, the STM must be propagated alongside the state.

1.1.2 Unscented Transform

An unscented transform (UT) can be used to propagate a state through a nonlinear function and recover the covariance [8]. Using the initial mean and covariance, a set amount of sigma points, usually sampled along the hyper-axes of the state uncertainty, can be generated that can better capture the initial non-Gaussian distribution. Each one of these sigma points can then be propagated through the nonlinear function and recombined to generate a new mean and covariance that captures information about the first two moments of the pdf. Derivation and further discussion of using unscented transforms is in [8]. Using UTs requires additional state propagations due to the additional sigma points but are able to capture second order effects.

1.1.3 Gaussian Mixture Models

Gaussian Mixture Models (GMMs) have been used to propagate state uncertainties through nonlinear equations of motion [9]. They work by assuming that any pdf can be approximated by a weighted combination of Gaussian pdfs with mean $\boldsymbol{\mu}$, covariance **P,** and weight α [10].

$$p_g(\boldsymbol{x}) \approx \sum_{i=1}^{N} \alpha_i p_i(\boldsymbol{x};\ \boldsymbol{\mu}_i, \boldsymbol{P}_i) \tag{6.5}$$

As the initial pdf is split into more GMMs (N), the individual covariances and weights shrink. Propagating each GMM through a nonlinear function allows for higher order effects to be accounted for but increases computational cost for each GMM generated. Since the variance along the splitting direction is the only one decreased, it is important to understand how the initial pdf is split because more useful splits can capture the final non-Gaussian and nonlinear effects better, which leads to a more accurate final pdf with less propagations.

1.1.3.1 Univariate Splitting Libraries

To approximate a pdf as a sum of individual pdfs, individual weights, means, and standard deviations are required. To derive these values, a performance index is used to determine how well the individual pdfs can be recombined into the original pdf. Based on how many final pdfs are desired, a set of weights, means, and standard deviations are derived and used [11].

1.1.3.2 Splitting Direction

The next step is to find which direction the univariate splitting library is to be applied. Given a desired direction **a,** it can be shown [11] that the resulting pdf can be represented by

$$\boldsymbol{\mu}_i = \boldsymbol{\mu} + \mu_i \boldsymbol{S}\hat{\boldsymbol{a}} \tag{7.6a}$$

$$\boldsymbol{P_i} = \boldsymbol{S}[\boldsymbol{I} + (\sigma_i^2 - 1)\hat{\boldsymbol{a}}\hat{\boldsymbol{a}}^{\boldsymbol{T}}]\boldsymbol{S}^{\boldsymbol{T}} \tag{8.6b}$$

$$\boldsymbol{\alpha_i} = \alpha\alpha_i \tag{9.6c}$$

where $\hat{\boldsymbol{a}}$ is

$$\hat{\boldsymbol{a}} = \frac{\boldsymbol{S}^{-1}\boldsymbol{a}}{\|\boldsymbol{S}^{-1}\boldsymbol{a}\|_2} \tag{10.6d}$$

The values of μ_i, α_i and σ_i are from the univariate splitting library. **S** is any square-root factor of **P** where $\mathbf{P} = \mathbf{S}\mathbf{S}^T$. It is common practice to have split the initial pdf in the direction of the largest eigenvalue of the covariance matrix [9], however it is more beneficial if the splitting direction can be of the highest nonlinearity.

1.2 Multidirectional Gaussian Mixture Models

Improvements on how to determine the optimal splitting direction for GMMs have been explored through Multidirectional Gaussian Mixture Models (MGMMs) [11]. Instead of choosing an arbitrary splitting direction, directions are analyzed for how nonlinear they are. Once the direction of highest nonlinearity is found, a split is performed along that direction using the univariate library. Then, each generated pdf can be split again along a different direction (or same direction). This process is done recursively until a desired number of GMMs is reached.

1.3 Element Space Selection

There has been no requirement placed on which element space uncertainty propagation needs to occur in. In fact, expressing uncertainty in certain elements such as equinoctial elements has shown a decrease in the nonlinearity during propagation [12]. This effect becomes more important as additional perturbations are added. Performing GMM splits in a different space is explored to determine if less splits are required to still capture the nonlinearity effects.

1.4 Probability of Collision

The final goal of proper and accurate uncertainty propagation remains probability of collision (Pc) calculations for two resident space objects (RSOs) in orbit. GMMs have been used to improve these calculations before [13]. There exist many methods to calculate

Pc between two RSOs [14, 15], all with varying degrees of assumptions and accuracy. However, since uncertainty propagation methods and not Pc calculation methods are the focus of this study, only one Pc method will be used for all scenarios. These various other Pc methods are logical extensions of this work.

Alfano's Pc method [16] assumes the relative motion between the two RSOs is linear for the encounter, each object can be modeled as a sphere with a combined hard body radius of R, positional errors are zero-mean, Gaussian, and constant for the encounter, and the relative velocity at the time of closest approach (TCA) is large enough where the encounter is brief. Obviously, these assumptions break down in many encounters.

Because GMMs are still Gaussian, Alfano's Pc method can be applied in an all on all method. Given GMMs of the primary (p) and secondary (s) RSOs with combined hard body radius R

$$P_c = \sum_{i=1}^{N_p} \sum_{j=1}^{N_s} \alpha_{pi} \alpha_{sj} f\{\boldsymbol{\mu}_{Pi}[t_{CA}(i,j)], \boldsymbol{P}_{Pi}[t_{CA}(i,j)], \boldsymbol{\mu}_{sj}[t_{CA}(i,j)], \boldsymbol{P}_{sj}[t_{CA}(i,j)], R\} \tag{11.7}$$

where $t_{CA}(i,j)$ is the TCA between the ith GMM of the primary object and the jth GMM of the secondary object. f{} is Alfano's Pc method.

Chapter 2: Improved MGMMs and Application to Probability of Collision

2.1 Improving MGMMs

To improve on MGMMs, the initial splitting technique is explored to optimize which directions are used to split, instead of using a predefined index based on the initial pdf. Equinoctial elements are also used to determine if a better split can be obtained.

2.1.1 Choosing the Best Splitting Direction

To determine which direction to split along, a measure of the nonlinearity is required. There exists many methods to determine this value [12], but equation 2.1 is used in this study because it allows for the nonlinear function to be evaluated at the time of closest approach (which is where it is most important) and retains more accuracy the further it is from the mean [12]. A second order divided difference can be used based on the direction **a.**

$$\mathbf{\Phi} = \frac{f(\boldsymbol{\mu}+h\sigma\hat{\boldsymbol{a}})+f(\boldsymbol{\mu}-h\sigma\hat{\boldsymbol{a}})-2f(\boldsymbol{\mu})}{2h^2} \tag{2.1}$$

where **f** is the nonlinear function that is being evaluated, $\sigma = \|\boldsymbol{a}\|_2\hat{\boldsymbol{a}}$, and h = $\sqrt{3}$ for a Gaussian initial distribution [17]. For the Pc application, **f** is propagating the initial state to TCA.

However, for splitting Gaussian mixtures (GMs), it is important to understand not only how nonlinear that direction is but also how important the GM is that is being split. A certain GM might have a very nonlinear direction but the corresponding weight of the mixture might be very low. On the other side, a highly weighted pdf could have a low nonlinear direction. To account for this and as a side effect to prevent ending up with very

low weighted pdfs, equation 2.1 is multiplied by the GM weight of the pdf being evaluated for splitting.

Given $\mathbf{x_0}$, $\mathbf{P_0}$, and a preset list of possible splitting directions $\mathbf{A} = \{\mathbf{a_1}, \mathbf{a_2}, \ldots, \mathbf{a_n}\}$, each direction is evaluated for how nonlinear it is using equation 2.1. Using a univariate splitting library of n number of elements, the initial pdf is then split along direction **a** with the highest nonlinearity index to form n GMMs. Then each n^{th} GMM is evaluated for each splitting direction in **A** for the nonlinearity index in equation 2.1 multiplied by the corresponding GM weight. The largest nonlinearity value of all possible directions in each n^{th} GMM is then found. The corresponding pdf is split along that direction to generate (n-1) more pdfs. This process is repeated until a certain threshold for **Φ** is met or a certain number of GMMs are generated.

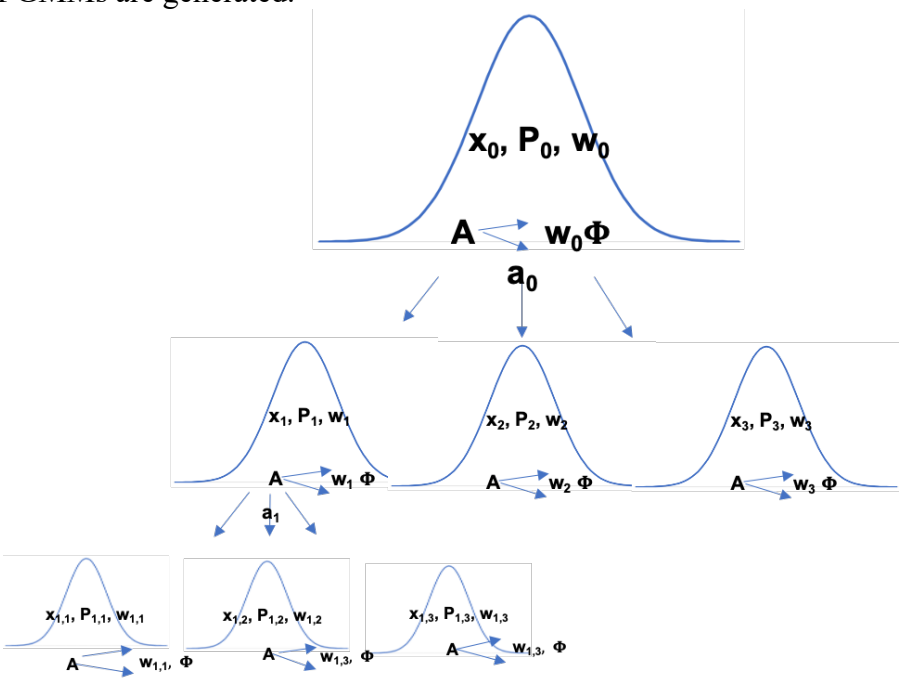

Figure 1: Splitting strategy for GMM based on GM weight and updated directions.

Figure 1 shows this splitting strategy with n = 3. In the first step, the initial pdf is analyzed along all directions in **A** and is split along the highest $w\mathbf{\Phi}$**.** The 3 formed GMMs are evaluated again and split along a direction of the first GMM. The next step would be to evaluate the 3 newly formed GMMs with the previous two not split to determine how to split again.

It is recognized that this splitting method is more computationally expensive than previous methods because it requires evaluation of the nonlinear function at every split for every direction of each GM. However, especially for two body dynamics, this computation time is negligible compared to the amount of equivalent Monte Carlo points needed to capture that nonlinearity. Additionally, this strategy can be tuned to use different nonlinearity indexes that do not rely on propagation but the Jacobian instead [12]. Plus, the knowledge gained from splitting one RSO can be applied to an RSO in a similar orbit.

2.1.2 Element Space Selection

To determine if equinoctial elements are a better representation of the nonlinear effects when performing the initial split, they are used alongside cartesian. The initial states and covariances are given in cartesian and are converted to equinoctial elements using an unscented transform. Once converted, they are split using the same splitting strategy in section 2.1.

2.2 PROPAGATION

States are propagated through two body dynamics per equation 1.2. Perturbations can be added, which could enhance some aspects of these new methods. All propagation is performed using symmetric sigma points [9]. For equinoctial elements, the sigma points generated are converted to cartesian and then propagated through the two body dynamics.

Once propagated to TCA, the sigma points are recombined to form the state and covariance in cartesian space since cartesian is required for Pc calculations.

2.3 Probability of Collision Calculations

For the linear and UT methods, each RSO's mean is propagated for a number of revolutions to generate an ephemeris. The minimum relative distance between the two RSOs is then found. A minimization scheme is then used to find the actual TCA once it has been bounded by the ephemeris times. With TCA known, the uncertainty can be propagated to this time. Pc is then calculated. TCA and Pc calculations were validated using [14].

The process is similar for the GMMs with the exception of it requiring an all on all calculation. Therefore, with the i^{th} GMM of RSO 1 and the j^{th} GMM of RSO 2, a new TCA is found near the original mean's TCA. The Pc calculation is then a weighted sum per equation 1.7.

Chapter 3: Results

The first test case explored was the GEO/GTO case from [13] with a TCA about 2.5 days after epoch. This was chosen because it's brief encounter is appropriate for the linear Pc method in use. The primary object in GEO is setup to have large uncertainty in the radial direction and the secondary object in a GTO will suffer from large nonlinear effects due to being in a very elliptic orbit.

The second test case explored was the HEO case from [14] (case 9). The linear methods are nearly 20% off. The HEO RSOs also are in a very stressing and nonlinear orbit which will really test how well the different methods can account for it.

Using test cases from previous papers allowed for comparison of methods as well as using the published Monte Carlo Pc values.

3.1 Initial Splitting Analysis

The same splitting directions from [13] were used with the eigenvectors of the covariance matrix added. They are the six eigenvectors, the inertial coordinates ($\mathbf{r_x}$, $\mathbf{r_y}$, $\mathbf{r_z}$, $\mathbf{v_x}$, $\mathbf{v_y}$, $\mathbf{v_z}$), and the radial, in-track, cross-track, and velocity directions ($\mathbf{r_r}$, $\mathbf{r_v}$, $\mathbf{r_h}$, $\mathbf{r_t}$, $\mathbf{v_r}$, $\mathbf{v_v}$, $\mathbf{v_h}$, $\mathbf{v_t}$). All splits use a 5-univariate library. Results are presented for just RSO 2 from the GEO/GTO case.

The MGMM strategy from [13] for the secondary object was to split in the $\mathbf{v_t}$ and $\mathbf{v_r}$ directions and all other directions 1 based on an evaluation of the initial nonlinearity.

The following are results for the new weighting and splitting MGMM scheme. The next 3 plots show the evolution of splitting direction as the number of allowable splits increases for the cartesian case.

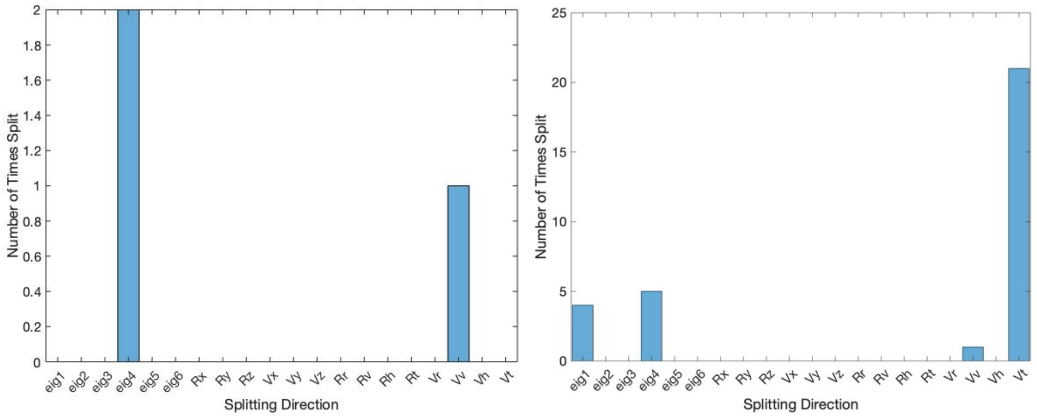

Figure 2: Splitting Directions as the Number of Allowable Splits Increases, RSO 2 of GEO/GTO Test Case, Cartesian

Initially, the new method found the 4th eigenvector of the covariance matrix to be more nonlinear than the $\mathbf{v_t}$ and $\mathbf{v_r}$ directions. But as this GM weight corresponding to the pdf with this nonlinear direction decreased, the $\mathbf{v_v}$ direction was split. As the number of allowable splits increased, the $\mathbf{v_t}$ direction dominated (as shown in [13]).

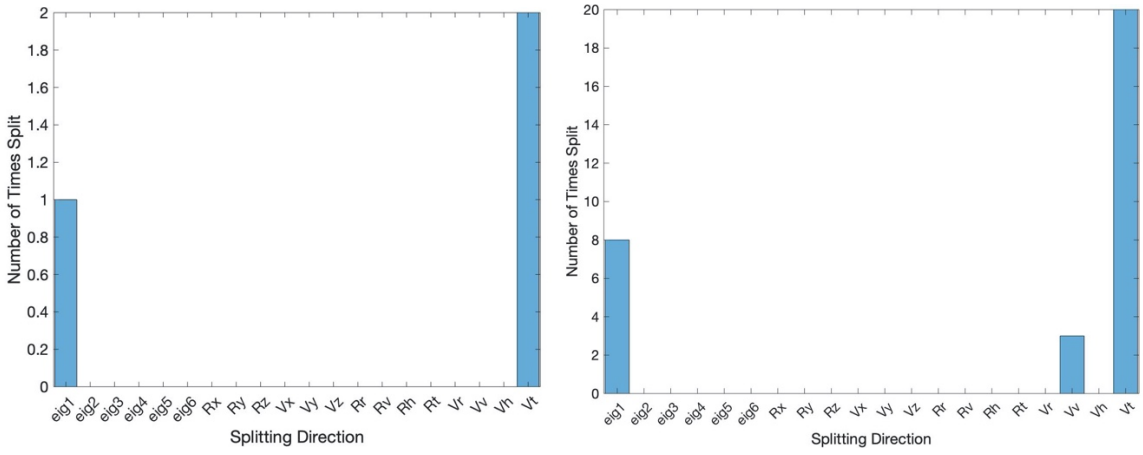

Figure 3: Splitting Directions as the Number of Allowable Splits Increases, RSO 2 of GEO/GTO Test Case, Equinoctial

Similar results are seen for the equinoctial splits, with the exception of a different eigenvector of the covariance matrix and equinoctial being split along the $\mathbf{v}_t$ initially.

The quality of the initial splits can further be assessed by propagating each GMM (cartesian improved, equinoctial improved, and MGMM) through two body dynamics for two days and compare with 2e6 Monte Carlo points. The plots have been converted into the RIC frame. The color of the GMM 3-sigma ellipses changes from blue to cyan as the GM weight decreases. Each GMM has 125 mixtures which equates to 1500 propagations with propagating using an UT.

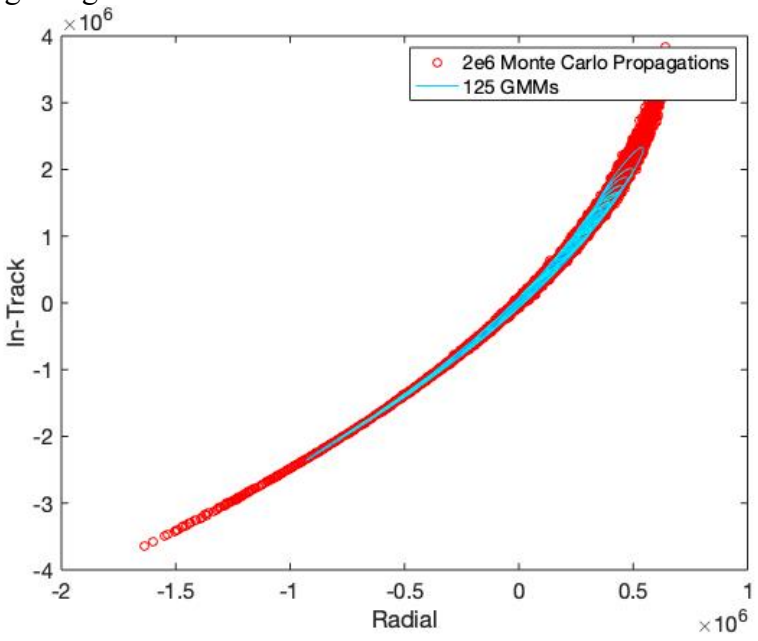

Figure 4: Cartesian, 125 GMM Propagated for 2 Days Compared with Monte Carlo Points for GEO/GTO Test Case

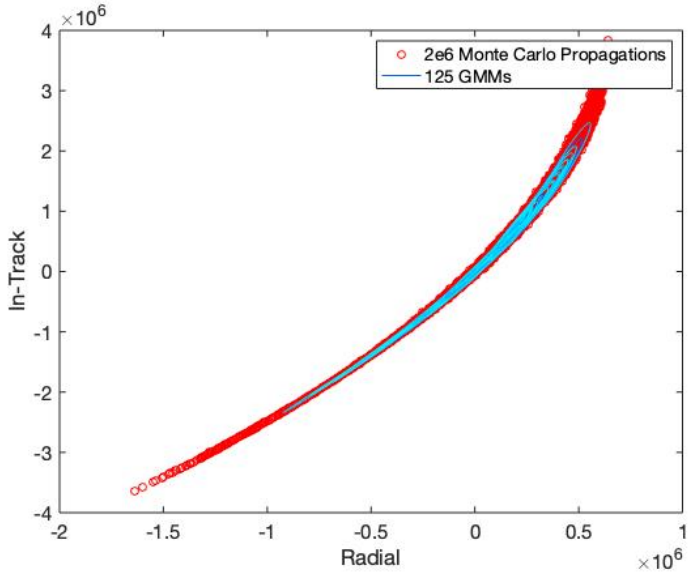

Figure 5: Equinoctial, 125 GMM Propagated for 2 Days Compared with Monte Carlo Points for GEO/GTO Test Case

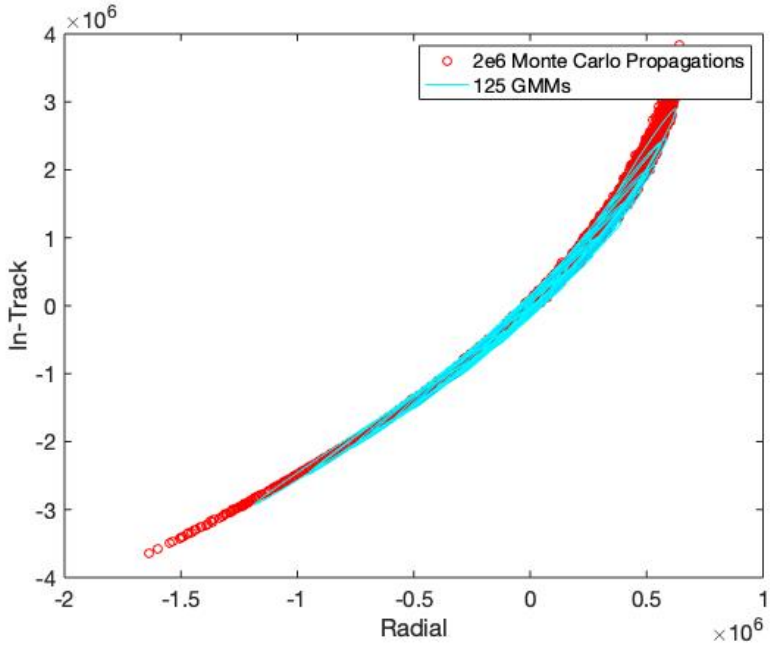

Figure 6: Normal MGMM, 125 GMM Propagated for 2 Days Compared with Monte Carlo Points for GEO/GTO Test Case

It is apparent that the MGMM method does a better job of capturing the tails of the nonlinear distribution. The equinoctial and cartesian (improved) MGMMs in Figures 5 and 6 tend to stay more concentrated and closer to the mean. This is because the MGMM has a preset splitting routine to follow, regardless of how important that direction actually is. This is seen in the color as well. The MGMM is a lot more cyan, meaning all of the weights are relatively low. Because all splits occur evenly across all available GMMs, the weights decrease at the same rate. The improved MGMMs have more blue mixed in meaning there still exists some GMs with large weights. These larger weights are not split because their possible splitting directions were not as nonlinear as other GMs. The tails for the improved MGMM cases are not represented as well, even with 125 mixtures. Similar results are seen in the cross-track direction.

Results are repeated for the second test case for two HEO RSOs.

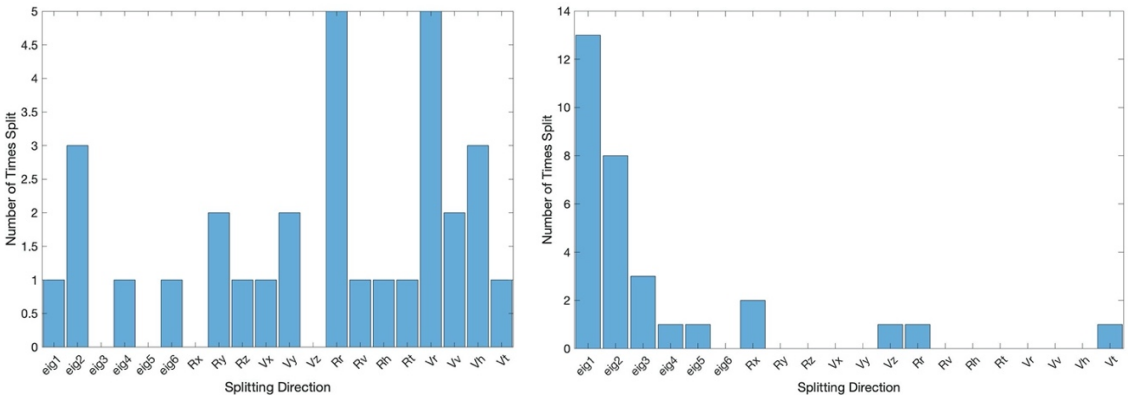

Figure 7: Splitting Directions for 125 GMM, Cartesian and Equinoctial, Respectively. RSO 2 of HEO test case.

Because of how nonlinear the orbit for this RSO is, the cartesian improved MGMM ends up distributing it's splits along almost every available direction, much like how the normal

MGMM is setup. However, the equinoctial is able to split mostly in the same few directions; the eigenvectors of the covariance matrix.

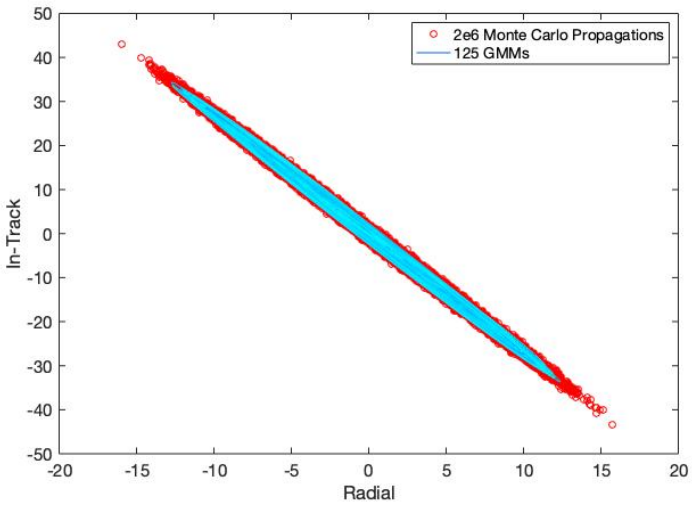

Figure 8: Cartesian, 125 GMM Propagated for 2 Days Compared with Monte Carlo Points for HEO Test Case

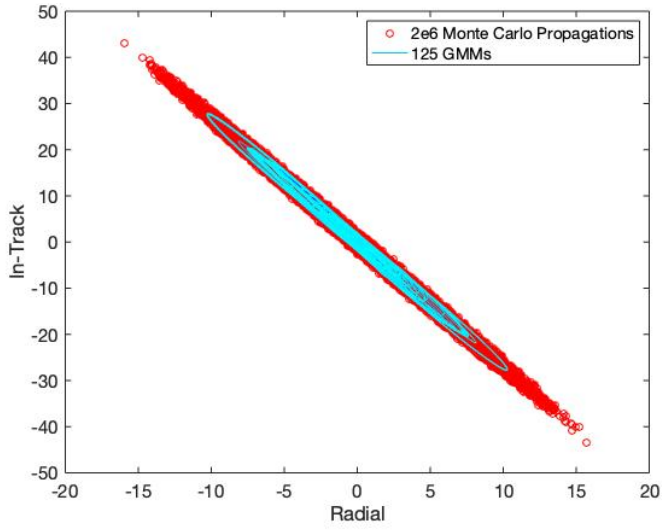

Figure 9: Equinoctial, 125 GMM Propagated for 2 Days Compared with Monte Carlo Points for GEO/GTO Test Case

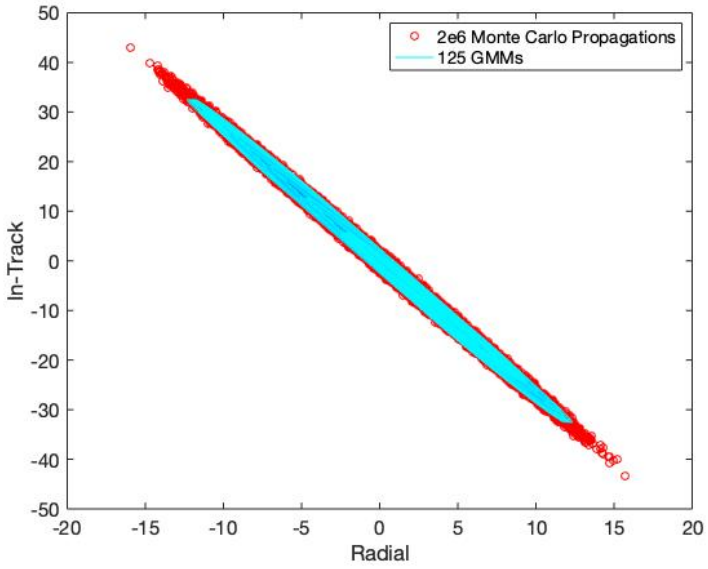

Figure 10: Normal MGMM, 125 GMM Propagated for 2 Days Compared with Monte Carlo Points for GEO/GTO Test Case

Figures 8-10 show how the different splitting strategies compare after two days of propagation for the HEO test case. The improved cartesian MGMM is very similar to the normal MGMM, while the equinoctial is more concentrated around the mean, leaving the tails unaccounted for.

3.2 Probability of Collision Results

The Pc results are presented for the same GEO/GTO case discussed in detail in section 3.1. This case was used because the linear and UT methods failed to be within 10%. It also allowed for easy comparison with the results of [13]. The number of propagations represent propagations of both RSOs as well as the individual sigma point propagations.

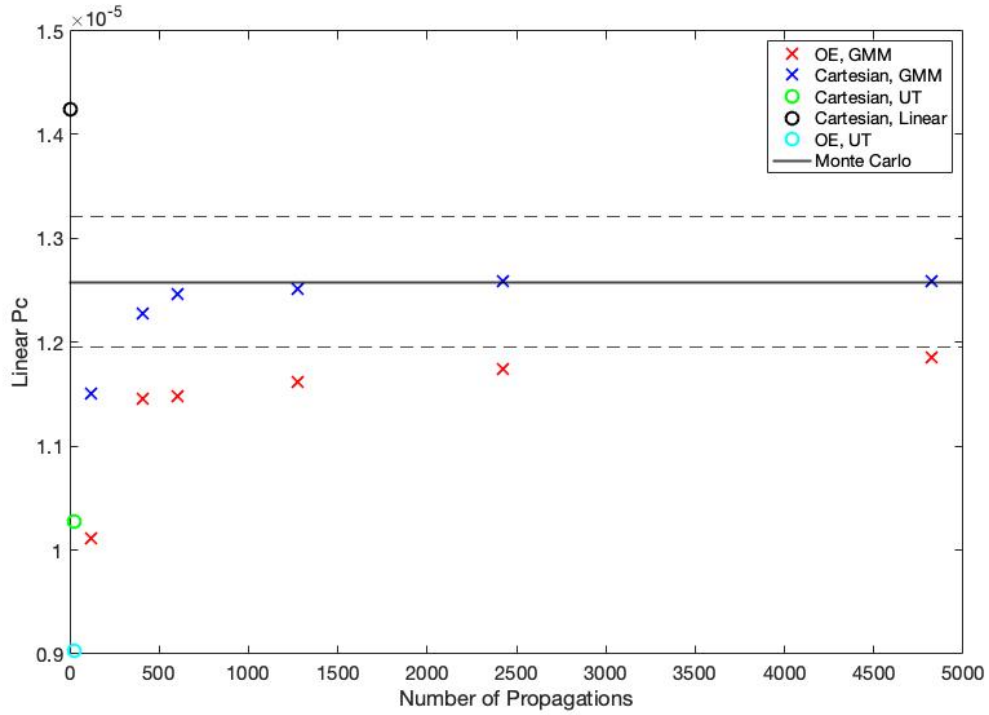

Figure 11: Probability of Collision Results for GEO/GTO Case

The dotted black lines represent a 5% error. The points designated as OE are the equinoctial elements. The improved MGMM cartesian method (blue x's) performs the best, passing the 5% mark in under 400 total propagations and reaching a stable Pc matching that of the MC at about 1400 propagations. Compared to Figure 5 of [13] where the MGMM method takes about 800 propagations to reach the 5% mark and closer to 10,000 propagations to reach that of the MC (unclear if it tapers off). The equinoctial elements do not perform as well as the cartesian improved MGMM method which aligns more with the results in [13]. This was not as expected and needs to be explored further.

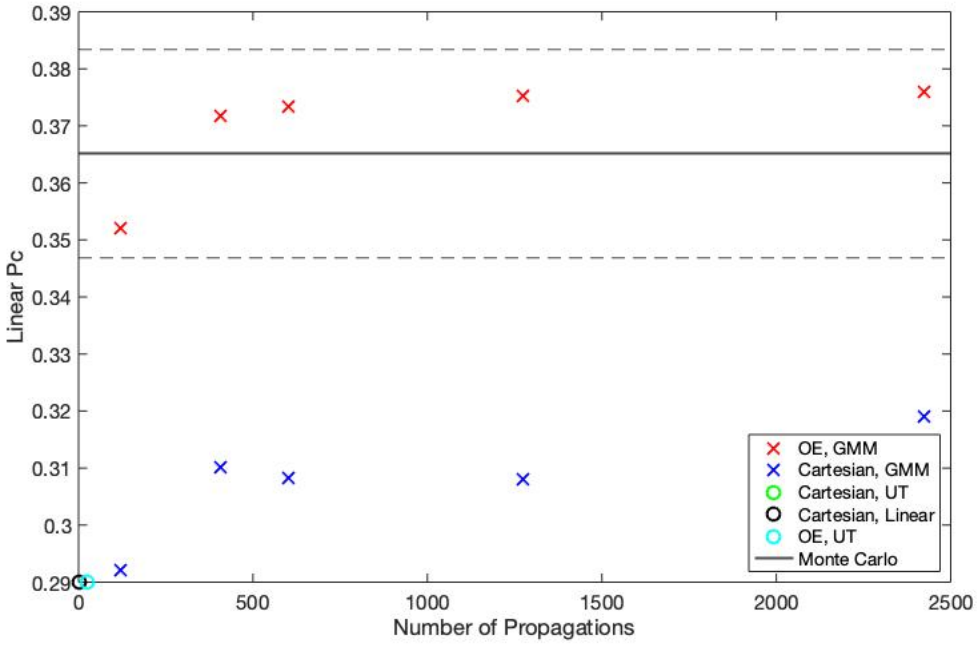

Figure 12: Probability of Collision Results for HEO Case

Figure 12 shows the results for the HEO case. It is of note how quickly the equinoctial MGMMs surpass the 5% mark, which matches how well the nonlinear dynamics are captured in Figure 9. However, they do not settle out on the MC value, showing that a lot more mixtures will be required to completely capture the effects. The cartesian MGMM do not surpass the 5% mark in a relatively short number of propagations because of their inability to model the higher order effects as seen Figures 8-10. This test case also has very nonlinear motion, including having an instantaneous Pc at epoch [14]. The assumptions underlying Alfano's Pc method start to break down, specifically the short encounter time.

Chapter 4: Conclusions

4.1 Splitting Directions

The updated splitting technique for GMMs where the nonlinearity index is calculated for each direction at each step for each GM, as well as taking into account the GM weights, proved to capture the majority of the nonlinearity effects of two body propagation with relatively few mixtures compared with previous research. However, as more mixtures are added, the improved methods tend to concentrate those mixtures around the mean and not around higher order effects. Therefore, that tails of the distribution do not get modeled without more and more mixtures. Larger splitting libraries need to be used to capture these effects.

4.2 Probability of Collision

With the improved methods, Pc calculations are able to be within 5% of the Monte Carlo with relatively few propagations. This applies even in very nonlinear encounters. However, as mentioned in section 4.1, the higher order effects are not modeled as well when more GMs are added, making it difficult to converge on the 100% solution. Limitations on the Pc method used also became apparent. These methods still remain valuable to the operator and analyst though; when performing conjunction assessment on the entire space catalog, a 95% answer is sufficient for the majority of the situations. Further analysis is required to achieve the 100% mark that is needed to maintain trust in the conjunction assessment process.

4.3 Future Work

Additional splitting techniques can be explored to account for the higher order effects to go from a 95% answer to a 100% answer. For instance, the size of the univariate

library can be set as proportional to the nonlinearity index instead maintaining it constant. This would allow for the tails of the nonlinear distribution to be better captured.

More work needs to be performed on the comparison between using cartesian and equinoctial elements. It is clear that in some very nonlinear cases, equinoctial elements outperform cartesian, while in other cases cartesian outperforms equinoctial. But it is difficult to determine where that line is drawn. Additional test cases are needed to be run.

Additional Pc calculations can be used including methods directly for GMMs. Maintaining the same Pc calculation allowed just different methods of splitting to be compared. However, there exists other, more accurate and specific to GMMs, that should be used.

AEGIS [9] can be used to better propagate the uncertainty. An initial split can be performed based on this research, but as propagation occurs and the entropy increases past a certain tolerance, the GM can be split again. Instead of choosing the largest eigenvalue direction, that split can be based on similar methods discussed here.

Hard body radius (R) remains an important variable in Pc calculations, but rarely in operations is that value accurately known. Future work could include analyzing the sensitivity of Pc calculations to changing R and whether GMMs can be used to decrease it.

And most importantly is the “now what” question. What does a Pc of 1e-4 actually mean? Is it worth the risk to save fuel costs and therefore operational lifetime? Is a maneuver required? What are the chances the maneuver makes the probability worse (either through miss-fire or wrong initial Pc calculation)? Is that maneuver globally optimum? That conjunction might have been avoided but now the satellite is on a collision course with another RSO. These are questions we do not want to figure out the hard way.

Bibliography

[1] Space Policy Directive-3, National Space Traffic Management Policy. Issued June 18, 2018.

[2] Pechkis, DL, Ns Pacheco, and Tw Botting. Statistical Approach to the Operational Testing of Space Fence. *IEE Aerospace And Electronic Systems* Magazine 31.11 (2016): 30–38.

[3] https://www.space-track.org. Accessed August 6, 2020.

[4] Brown, Chase, Stauch, Jason, and Iyer, Shiva. Multi-Source Resident Space Object State Validation and Fusion. Presented at IAA-UT-Space Traffic Management Conference. February 19, 2020.

[5] S. Alfano. Review of conjunction probability methods for short-term encounters. In AAS/AIAA Space Flight Mechanics Meeting, Sedona, Arizona, AAS 07-148, 2007.

[6] Tapley, Byron D., Bob E. Schutz, and George H. Born. Statistical Orbit Determination Amsterdam ;: Elsevier Academic Press, 2004.

[7] Bani Younes, A. (2019). Exact Computation of High-Order State Transition Tensors for Perturbed Orbital Motion. Journal of Guidance, Control, and Dynamics, 42(6), 1365–1371. https://doi.org/10.2514/1.G003897

[8] Julier, S., and Uhlmann, J. K. Unscented Filtering and Nonlinear Estimation, Proceedings of the IEEE, Vol. 92, No. 3, 2004, pp. 401–402. doi:10.1109/JPROC.2003.823141.

[9] K. J. DeMars, R. H. Bishop, and M. K. Jah. Entropy-based Approach for Uncertainty Propagation of Nonlinear Dynamical Systems. Journal of Guidance, Control, and Dynamics, 36(4):1047–1057, 2013.

[10] Daniel L. Alspach and Harold W. Sorenson. Nonlinear Bayesian Estimation using Gaussian Sum Approximations. IEEE Transactions on Automatic Control, 17(4):439–448, 1972.

[11] Vittaldev, V., and Russell, R. P., Multidirectional Gaussian Mixture Models for Nonlinear Uncertainty Propagation, Computer Modeling in Engineering & Sciences, March 2016, http://www.techscience.com/cmes/.

[12] J. L. Junkins, M. R. Akella, and K. T. Alfriend. Non-Gaussian Error Propagation in Orbital Mechanics. Journal of the Astronomical Sciences, 44(4):541–563, 1996.

[13] V. Vittaldev and R. P. Russell. Collision Probability using Multidirectional Gaussian Mixture Models, aas 15-394. In AAS/AIAA Space Flight Mechanics Meeting, Williamsburg, VA, January 11-15, 2015.

[14] Salvatore Alfano. Satellite Conjunction Monte Carlo Analysis. In AIAA Space Flight Mechanics Meeting, AAS 09-233, 2009.

[15] V. Coppola. Including Velocity Uncertainty in the Probability of Collision Between Space Objects. In AAS/AIAA Spaceflight Mechanics Meeting, Charleston, SC, AAS 12-247, 2012.

[16] Alfano, S. A Numerical Implementation of Spherical Object Collision Probability, Journal of the Astronautical Sciences, Vol. 53, No. 1, January-March 2005, pp. 103-109.

[17] Norgaard, M., Poulsen, N. K., and Ravn, O.. New Developments in State Estimation for Nonlinear Systems, Automatica, Vol. 36, No. 11, 2000, pp. 1627–1638.